BMC Biology

RESEARCH ARTICLE

Open Access

A dynamic transcriptional cell atlas of testes development after birth in Hu sheep

Jie Su[1], Yanyan Yang[2], Daqing Wang[3], Hong Su[3], Feifei Zhao[3], Chuanqiang Zhang[4], Min Zhang[3], Xiunan Li[2,3], Tingyi He[2], Xihe Li[4,5], Ying Tian[2], Biao Song[6,7], Chao Chen[7], Yongli Song[5*] and Guifang Cao[3*]

Abstract

Background Testes development is a fundamental process in sexual development and reproduction. The testes undergo dramatic structural changes during development, including the proliferation and differentiation of somatic cells such as Sertoli cells, Leydig cells, and myoid cells, as well as the maturation of spermatogonia. However, little is known about the onset of spermatogenesis and cell proliferation and maturation in the spermatogonial niche in large animals.

Results We used single-cell RNA sequencing (scRNA-seq) to profile nearly 100,000 cells from Hu sheep testes across seven developmental stages (birth, prepuberty, puberty, and adulthood). We constructed single-cell transcriptomic atlases and identified distinct spermatogonial subtypes, revealing dynamic gene expression patterns during spermatogenesis. Notably, we observed that two distinct Sertoli cell states converge into a mature population during puberty. Additionally, we identified a common prepubertal progenitor for Leydig and myoid cells, with Leydig cells transitioning through progenitor and immature stages before reaching maturity.

Conclusions Our study provides a comprehensive atlas of Hu sheep testes development, revealing key insights into the dynamic changes and regulatory mechanisms of spermatogenesis and somatic cell maturation from birth to adulthood. These findings offer new perspectives on testicular development in large mammals and support future research on reproductive biology and breeding strategies.

Keywords Single-cell RNA sequencing, Hu sheep, Testes, Spermatogenesis

*Correspondence:
Yongli Song
songyongli625@163.com
Guifang Cao
guifangcao@126.com
[1] Medical Neurobiology Laboratory, Inner Mongolia Medical University, Hohhot 010030, China
[2] Inner Mongolia Academy of Agricultural & Animal Husbandry Sciences, Hohhot 010000, China
[3] Key Laboratory of Animal Embryo and Development Engineering of Universities of Higher Learning, Inner Mongolia Agriculture University, Hohhot 010018, China
[4] Inner Mongolia Saikexing Institute of Breeding and Reproductive Biotechnology in Domestic Animal, Hohhot 011517, China
[5] Research Center for Animal Genetic Resources of Mongolia Plateau, Inner Mongolia University, Hohhot 010021, China
[6] Inner Mongolia University of Finance and Economics, Hohhot 010051, China
[7] Medical Intelligent Diagnostics Big Data Research Institute, Hohhot 010020, China

Background

The main function of the testes is to produce sperm and androgens. In mammals, the germ cells and somatic cells within the seminiferous tubules undergo a variety of changes during testicular development [1]. Spermatogenesis involves the differentiation of adult spermatogonial stem cells (SSCs) into mature sperm through a complex developmental process regulated by the testicular niche. SSCs originate from the basal membrane of the seminiferous tubules and play a critical role in maintaining male fertility in different species [2]. In addition to SSCs and spermatocytes, other somatic cells, including Leydig cells, myoid cells, and Sertoli cells, are involved in spermatogenesis and constitute the microenvironment, or niche, of the testes, which is essential for regulating normal spermatogenesis [3]. Sertoli cells are in direct contact with germ cells and perform a supportive function [4]. Leydig cells, located in the interstitial space between the seminiferous tubules, primarily function to secrete androgens [5]. Myoid cells, which surround the seminiferous tubules, possess smooth muscle-like characteristics and are intimately involved in spermatogenesis and the intratesticular transport of immotile sperm [6].

Research on postnatal structural changes during testes development, including the proliferation and maturation of somatic cells and the onset of spermatogenesis, has primarily focused on mice and humans [7–13]. In contrast, research on large animals, particularly sheep, is scarce. Specifically, there is limited knowledge about spermatogenesis, Sertoli cell heterogeneity, and molecular-level interactions with other cell types in sheep.

Hu sheep are a famous multiparous breed that primarily lives in the eastern coastal provinces at low altitudes in China [14]. The testes development in Hu sheep includes a fetal stage, infant stage, pubertal stage (sexual maturation), and adult stage. Hu sheep usually begin puberty at 3 months of age, but spermatogenesis is not initiated at this stage. Sexual maturation begins at 6 months of age; it is at this timepoint that the production of spermatozoa is initiated. Hu sheep can mate at 8 months of age and achieve body maturity at 12 months of age [15].

scRNA-seq approaches have been applied to investigate adult spermatogenesis in humans and mice. Lukassen et al. constructed the first comprehensive, unbiased single-cell transcriptome of mouse spermatogenesis and depicted the distinct single-cell transcriptional features of the aged mouse testes [16, 17]. Hermann et al. mapped the development of spermatogonia, spermatocytes, and spermatids in detail by comparing different types of germ cells in humans and mice [18]. After defining the developmental trajectory of mouse germ cells, Ernst et al. focused on the reactivation of the X chromosome in the postmeiosis period [19]. Guo et al. analyzed the dynamic changes in human adolescent and adult testicular cells and reported two distinct cell states: immature Sertoli cells and progenitor cells, namely Leydig cells and myoid cells [11].

In this study, we used the 10×Chromium Single Cell Controller (10×Genomics) platform to perform scRNA-seq on Hu sheep testes at 7 developmental stages from birth to adulthood. The workflow of the analysis is shown in Additional file 1: Fig. S1. Our study reveals changes in germline stem cells and complex modulations of the somatic niche in the sheep testes from birth to adulthood, as well as candidate factors and pathways that regulate somatic cell development. The results of this study reveal the complex changes that occur in the testes from birth to adulthood and provide technical support for sheep breeding research.

Results

Single-cell transcriptomes of Hu sheep testes reveal cell types and marker genes

To identify the cell types and marker genes involved in testes development after birth in Hu sheep, we obtained testes tissues from Hu sheep at 0, 30, 90, 180, 270, 360, and 540 days after birth. To systematically investigate both germ cell and somatic cell development after birth, we prepared single-cell suspensions from these testes tissues and performed scRNA-seq via the 10×Genomics platform (Fig. 1A, Additional file 2). After filtering out poor-quality cells, 12,465, 12,849, 12,388, 10,008, 16,827, 13,615, and 12,035 cells remained for subsequent analysis from samples obtained at 0, 30, 90, 180, 270, 360, and 540 days after birth, respectively (Additional file 3). Next, we clustered the cell types through uniform manifold approximation and projection (UMAP) analysis and unbiased computational informatic analysis (Fig. 1B). Germline-specific markers were expressed solely in clusters 1–3, with cluster 1 consisting of spermatogonia ($UTF1^+$), cluster 2 consisting of spermatocytes ($SYCP3^+$), and cluster 3 consisting of spermatids ($IZUMO1^+$ and $SPEM2^+$). Clusters 4–8 correspond to a heterogeneous mixture of Sertoli cells (cluster 4; $SOX9^+$), Leydig and myoid cells (cluster 5; $ACTA2^+$ and/or $MYH11^+$), vascular smooth muscle cells (VSMs) (cluster 6; $RGS5^+$), macrophages and T cells (cluster 7: $CD14^+$ and $CD3E^+$), and endothelial cells (cluster 8; VWF^+) (Fig. 1C and Additional file 4: Fig. S2). In total, according to the gene expression dynamics of the marker genes, we identified 10 clusters of cells in the Hu sheep testes, including male germ cells ranging from spermatogonia to spermatids and four types of testicular somatic cells.

The differential gene expression levels in the Hu sheep testes at different developmental stages were analyzed.

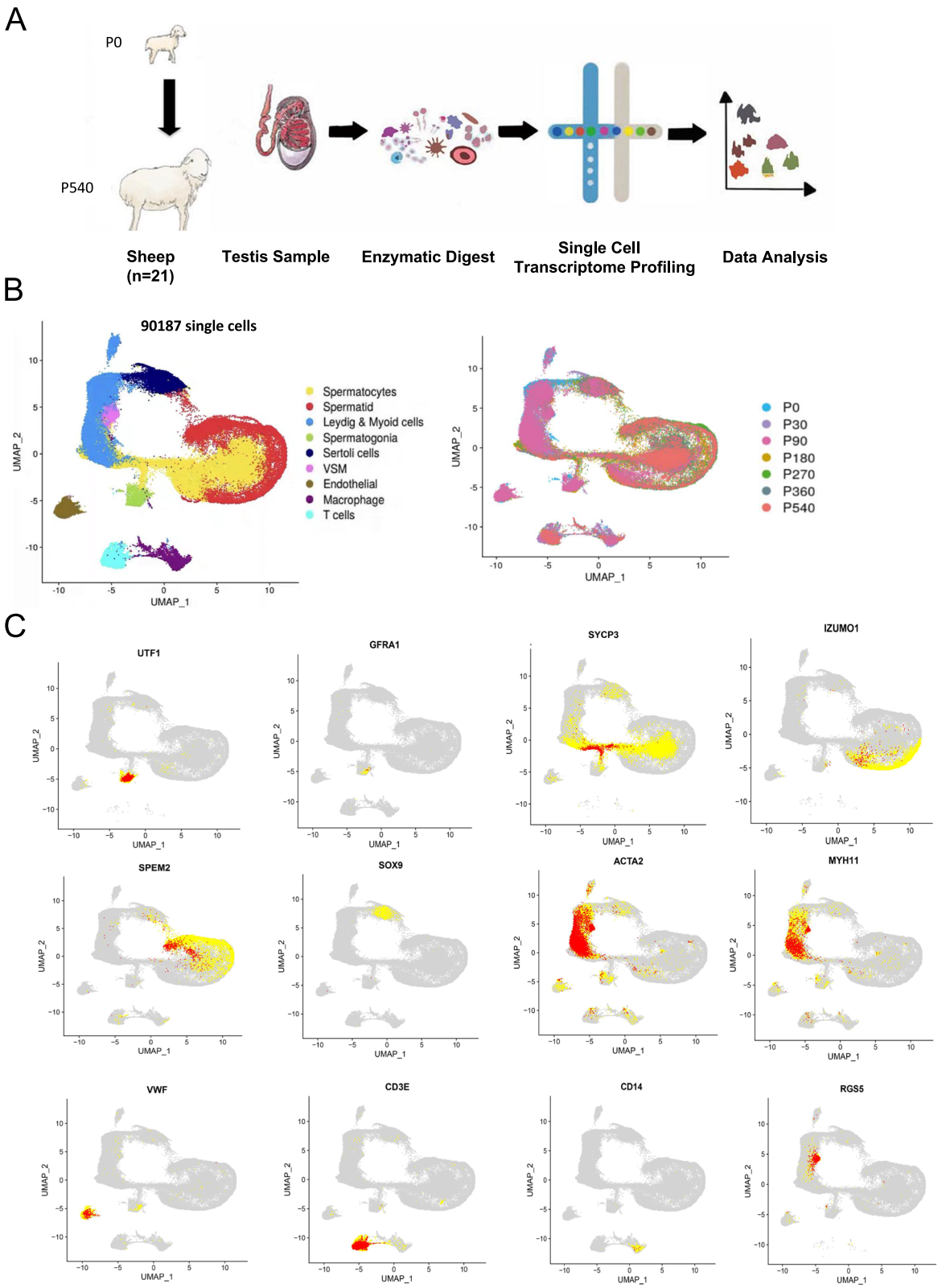

Fig. 1 Single-cell transcriptome profiling of testes in Hu sheep at different developmental stages. **A** Schematic illustration of the experimental workflow. **B** UMAP and clustering analysis of single-cell transcriptome data. Each dot represents a single cell in the UMAP plot. **C** Expression patterns of selected markers projected on UMAP. For each cell cluster, one cell marker is shown in the main figure, accompanied by further markers in Supplementary Fig. 2

The results revealed that the number of down- and upregulated genes at 30 days vs. 0 days and 90 days vs. 30 days was lower than that at the next four developmental stages (Additional file 5: Fig. S3).

Consistent with prior observations [20], our histological examination revealed significant changes in morphology and composition. At 90 days, spermatocytes were identified in the testes, whereas at 180 days, spermatids and sperm were observed, and the seminiferous tubule lumen appeared (Additional file 6: Fig. S4).

Spermatogonial proliferation and differentiation from birth to adulthood in Hu sheep

To investigate changes in germ cell composition after birth in Hu sheep, we conducted further analysis of germ cells following specific reclustering of initial clusters 1–3. First, using marker genes identified in humans and mice, we assigned germ cells into four broad developmental stages: undifferentiated spermatogonia (GFRA1$^+$ and UCHL1$^+$), differentiated spermatogonia (KIT$^+$), early primary spermatocytes (ZCWPW1$^+$), late primary spermatocytes (PIWIL1$^+$), and spermatids (TEX101$^+$ or PRM1$^+$) (Fig. 2A, B).

After germ cell reclustering, we analyzed the relative germ cell composition at different stages of testes development. The germ cells observed in samples taken at birth consisted solely of undifferentiated spermatogonia (Fig. 2C). Among the samples obtained at 30 days after birth, a high proportion of undifferentiated and differentiated spermatogonia were observed. Spermatocytes and sperm were observed in samples obtained 90 and 180 days after birth, respectively (Fig. 2C). Notably, spermatogonia were relatively rare in the samples obtained at 0 and 30 days after birth, comprising 3.2 to 3.4% of total testicular cells, and the relative proportion of spermatogonia increased to 11.8% in the samples taken 90 days after birth. The germ cell composition of the samples obtained 180 days after birth resembled that of the adult samples, indicating sexual maturity (Additional file 7: Fig. S5A).

To further verify the developmental pattern of the germ cells, we performed immunofluorescence (IF) of Hu sheep testes obtained at the same timepoints. First, staining with UCHL1 revealed that undifferentiated spermatogonia began to appear from 0 to 540 days (Fig. 2D). Next, we examined the proliferation and differentiation of undifferentiated spermatogonia using the markers PCNA and KIT, respectively. We observed that the proliferation of undifferentiated spermatogonia began after birth, and differentiation was observed at 30 days (Additional file 7: Fig. S5B and C). We also examined the presence of active meiosis using the meiotic marker SYCP3 and observed significant levels of staining only after 90 days (Additional file 7: Fig. S5D).

Taken together, these findings suggest that the spermatogonia in Hu sheep can be divided into undifferentiated and differentiated spermatogonia. Differentiated spermatogonia were observed at 30 days, and the proportion of spermatogonia was highest at 90 days and gradually stabilized in adulthood.

Pseudotime and clustering analyses reveal dynamic gene expression patterns during spermatogenesis

Spermatogenic cells undergo ordered and complex changes during spermatogenesis. We used Monocle for pseudotime analysis to understand the relationships between the different cell types. The germ cell clusters were arranged over pseudotime from left to right to form a continuous curve (Fig. 3A and B). Next, we performed clustering analysis of genes while fixing the order of the cells (columns) along the pseudotime axis, which revealed distinct gene cohorts (Fig. 3C and Additional file 8). The top 10 differentially expressed genes (DEGs) in the testicular germ cells of Hu sheep are shown in Additional file 9. SMC3, MIF, and PTMA were specifically expressed in spermatogonia; TEX101, SEC11C, and HIST1H1T were highly expressed in early primary spermatocytes; YNE2, CCDC173, and CFAP100 were highly expressed in late primary spermatocytes. PRESS37, C10orf120, and RNF151 were highly expressed in spermatids.

Gene Ontology (GO) analysis of these clusters revealed dynamic changes in genes during germ-cell development, indicating that the cellular and metabolic sequence of events, consistent with well-organized germline development, occurred in these cells. The results revealed that the upregulated genes were expressed in spermatogonia and that their molecular functions were enriched in the cell cycle in early and late primary spermatocytes, suggesting that the genes upregulated in these two cell types are primarily related to meiosis (Fig. 3C and Additional file 10). Functional enrichment analysis of genes upregulated in spermatids revealed that they were mainly involved in spermatogenesis (Fig. 3C).

We analyzed the changes in the expression of several genes during spermatogenesis, as shown in Fig. 3D. The results indicated that UTF1, UCHL1, and TKTL1 were expressed mainly in spermatogonia, while SYCP3, PIWIL1, and HELLS had higher expression levels in spermatocytes than in spermatids.

Identification of Sertoli cell heterogeneity and stages during maturation in Hu sheep

We next explored Sertoli cell development in Hu sheep. Clustering analysis revealed two large Sertoli clusters and one smaller cluster (Fig. 4A). Cell cycle analysis revealed

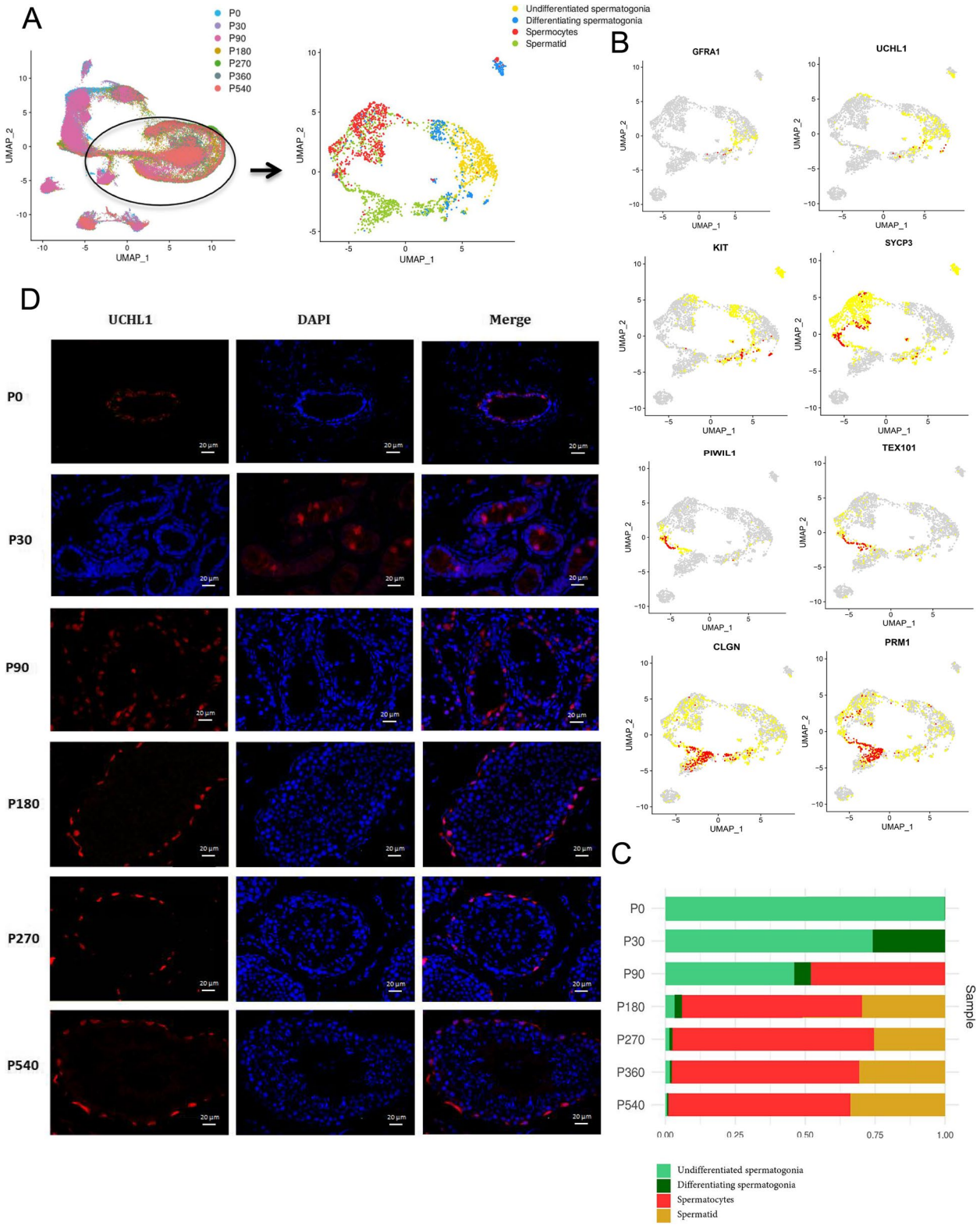

Fig. 2 Distinct phases of spermatogonial proliferation and differentiation in Hu sheep testes form birth to adulthood. **A** Focused UMAP and clustering analysis of germ cells reveals the developmental progression of spermatogenesis from birth to adulthood. **B** Expression patterns of known spermatogenic markers projected onto the UMAP plot. **C** Relative proportion of single cells at different spermatogenic stages in the analyzed samples. **D** IF for UCHL1^{+} cells in the Hu sheep testes during different developmental stages. Scale bar = 20 μm

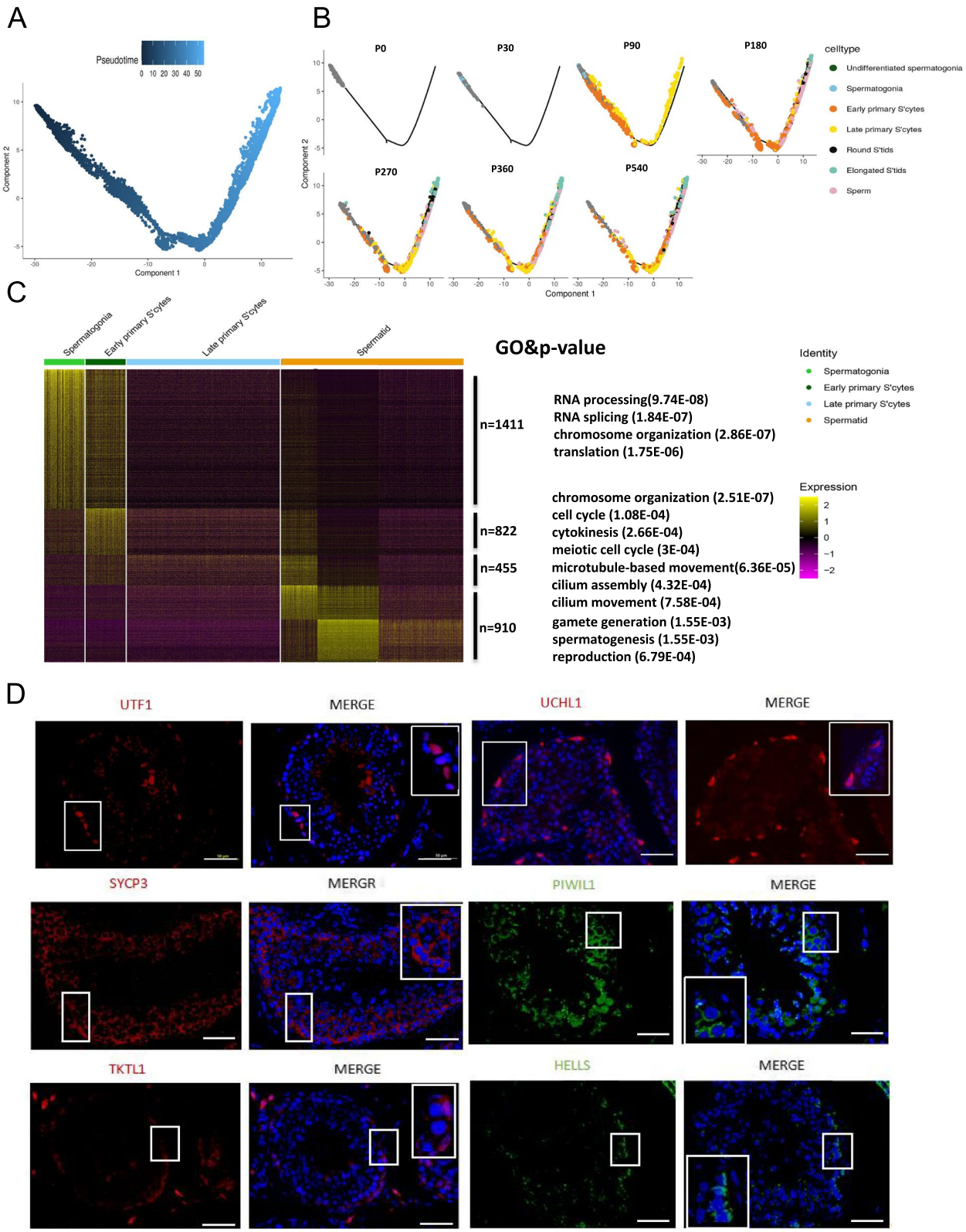

Fig. 3 Gene expression dynamics during spermatogenesis. **A** Pseudotime trajectory (Monocle analysis) of the germ cells. Cells are colored based on the predicted pseudotime. **B** Deconvolution of the Monocle pseudotime plot according to ages/donors of origin. **C** Heatmap showing the expression of differentially expressed genes across germ cell populations. Horizontal ribbons depict the identified cell types. Representative GO terms and *P* values are shown for each cell type. **D** IF analysis of the localization of UTF1, UCHL1, SYCP3, HELLS, and TKTL1 in Hu sheep testes

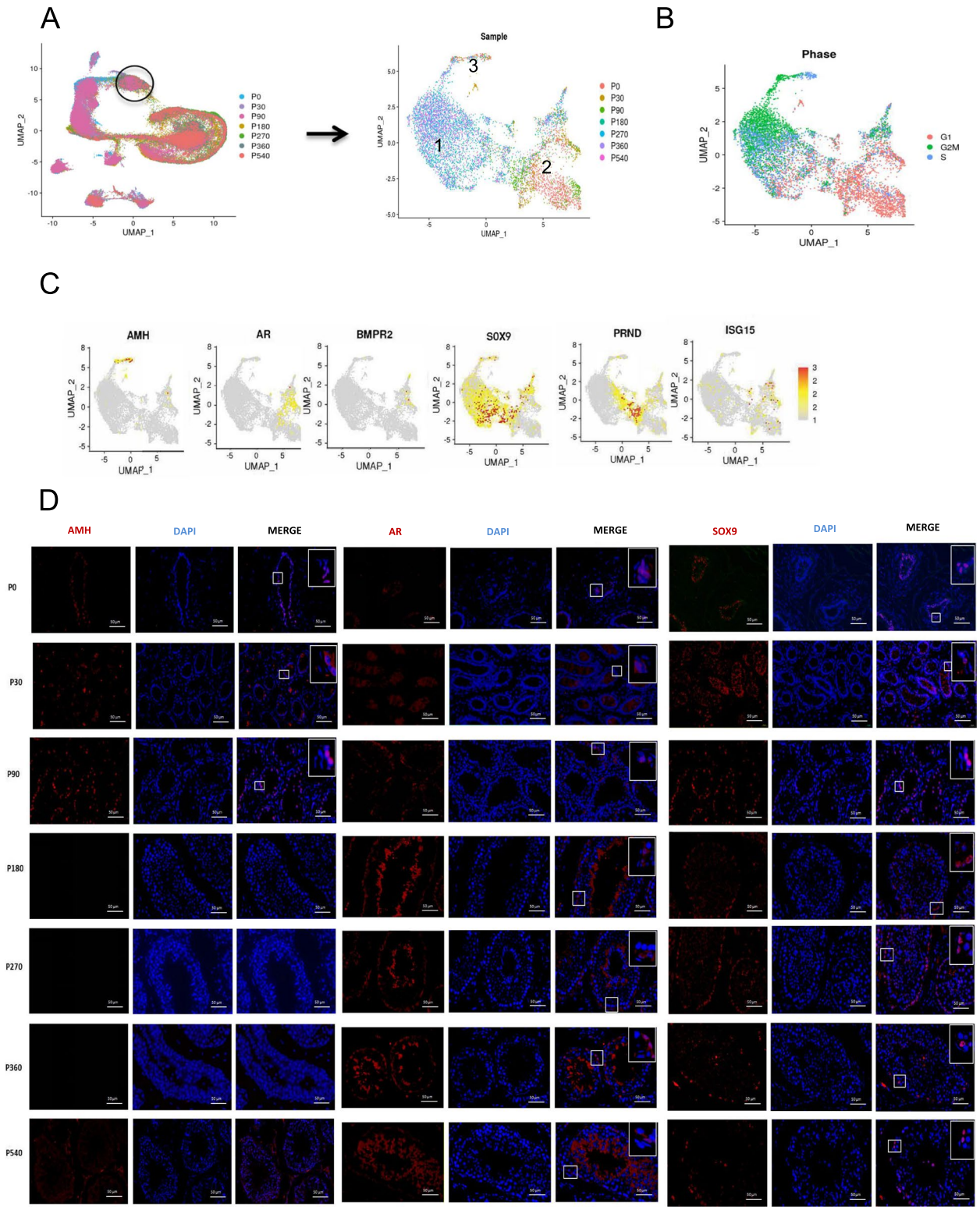

Fig. 4 Identification of Sertoli states in Hu sheep testes. **A** Focused UMAP and clustering analysis of Sertoli cells, with cells colored by age. **B** Focused UMAP and reclustering analysis of Sertoli cells, with cells colored according to their cell cycle phase (G1/S/G2). **C** Expression patterns of representative markers projected onto the UMAP. **D** IF for AMH^+, AR^+, and $SOX9^+$ cells in Hu sheep testes during different developmental stages. Scale bar = 50 μm

that the largest cluster (at right) contained cells from the 0 to 90-day samples and displayed a G1 phase bias, whereas the large cluster (at left) was composed mainly of cells from the 180 to 540-day samples (Fig. 4B). Monocle pseudotime analysis revealed that Sertoli cells at 0 and 30 days exist in two distinct states, termed immature 1 and 2. Notably, a third type of Sertoli cell (mature Sertoli cells) was observed at 90 days (Fig. 4C and Additional file 11: Fig. S6A and B). IF staining for AMH, AR, and SOX9 confirmed the developmental process of Sertoli cells (Fig. 4D).

After birth, most Sertoli cells were classified as immature 1 or 2, and the ratio between the numbers of immature 1 and 2 Sertoli cells decreased with age, reaching the lowest point at puberty (Additional file 11: Fig. S6C). Mature Sertoli cells do not appear until puberty, after which their proportion remains stable throughout adulthood. Co-staining for SOX9 and PCNA revealed that $SOX9^{+}/PCNA^{+}$ cells could be observed in the Hu sheep testes at 0–90 days but not after 180 days, indicating that Sertoli cells have the ability to proliferate after birth but do not proliferate during adulthood (Additional file 11: Fig. S6D). Notably, these results indicate that the progressive maturation of Sertoli cells begins at an early age and reaches a stable state in late puberty.

Next, we analyzed the differential gene expression during Sertoli maturation and identified genes whose expression differed between the immature and mature stages. A Venn diagram of the DEGs was constructed (Additional file 11: Fig. S6E). GO analysis revealed enrichment for different terms in immature 1, immature 2, and mature Sertoli cells (Additional file 11: Fig. S6F and Additional files 12 and 13). The terms enriched in immature 1 cells were translation, cellular response to transforming growth factor beta stimulus, and positive regulation of the apoptotic process. The terms enriched in immature 2 cells were translation, mitotic cell cycle process, and sister chromatid segregation. In mature Sertoli cells, the enriched terms were sexual reproduction, spermatogenesis, and multicellular organism reproduction.

Taken together, these data reveal that Sertoli cells undergo consecutive developmental stages that coincide with changes in their gene expression profile and proliferation.

Leydig and peritubular myoid cells

Reclustering of Leydig and myoid cells revealed that the cells expressed known markers of fetal Leydig cells (FLCs) and their precursors (e.g., MAFB and NR4A1; Fig. 5A and B), as well as heterogeneous markers typically associated with both adult Leydig cells (ALCs) and myoid cells (e.g., APOE and MYH11, respectively). Monocle pseudotime analysis showed that Leydig and myoid cells differentiated from common progenitor cells (Fig. 5C). Progenitor cells, FLCs, and myoid cells were observed from 0 to 90 days after birth. ALCs were first observed in samples obtained 180 days after birth and were predominant after sexual maturity, at which time the progenitor cell populations disappeared (Fig. 5D and E).

We next identified lineage-specific genes and programs, yielding approximately 3000 DEGs (Fig. 5F). Precursor cells express specific genes associated with transcription; as cells progress towards the myoid lineage, oxidative phosphorylation and reproduction-related genes become expressed (Fig. 5F). In contrast, cells that progress through the Leydig lineage express genes involved in secretion, consistent with the known steroidogenic function of these cells (Fig. 5F).

Overall, Leydig and myoid cells possess bipotential progenitors before puberty, and Leydig cells progress through progenitor and immature stages before achieving the terminally differentiated adult stage.

Signaling pathways regulating testes development

To explore germ cell–niche and niche–niche interactions, we examined signaling factor relationships. We observed dynamic and cell type-specific expression of genes encoding ligands, inhibitors, receptors, and gene targets from multiple signaling pathways. Retinoic acid (RA) induces germ cell differentiation. Enzymes for RA synthesis, ALDH1A1 and ALDH1A3, are specifically expressed in Sertoli cells after birth. STRA8, an RA target gene, is expressed in spermatogonia and is involved in the spermatogonia-to-spermatocyte transition (Fig. 6A). Interestingly, the WNT ligand WNT2B was expressed in Leydig cells, whereas the WNT2B receptor (FZD3) was confined to spermatogonia and early and late primary spermatocytes, suggesting a role for WNT2B in spermatogonial differentiation and meiosis in Hu sheep (Fig. 6B). FGF9 was expressed in spermatid cells, and its receptors FGFR1 and FGFR2 were expressed in spermatogonia, indicating that FGF signaling activity in Hu sheep testes persists through adulthood (Fig. 6C). We observed that Sertoli and Leydig cells expressed high levels of INHA, INHBB, and INHBA in samples obtained after 90 days, which led to increased activin and decreased inhibin activity in adulthood. We observed that activin receptors (ACVR1B and BMPR1B) are expressed in spermatogonia, whereas key inhibitors of activin signaling (FST and BAMBI) are specifically expressed in undifferentiated spermatogonia. These results indicate that the activin pathway is selectively inhibited in slowly self-renewing and undifferentiated spermatogonia but is active in proliferating and differentiated spermatogonia (Fig. 6D).

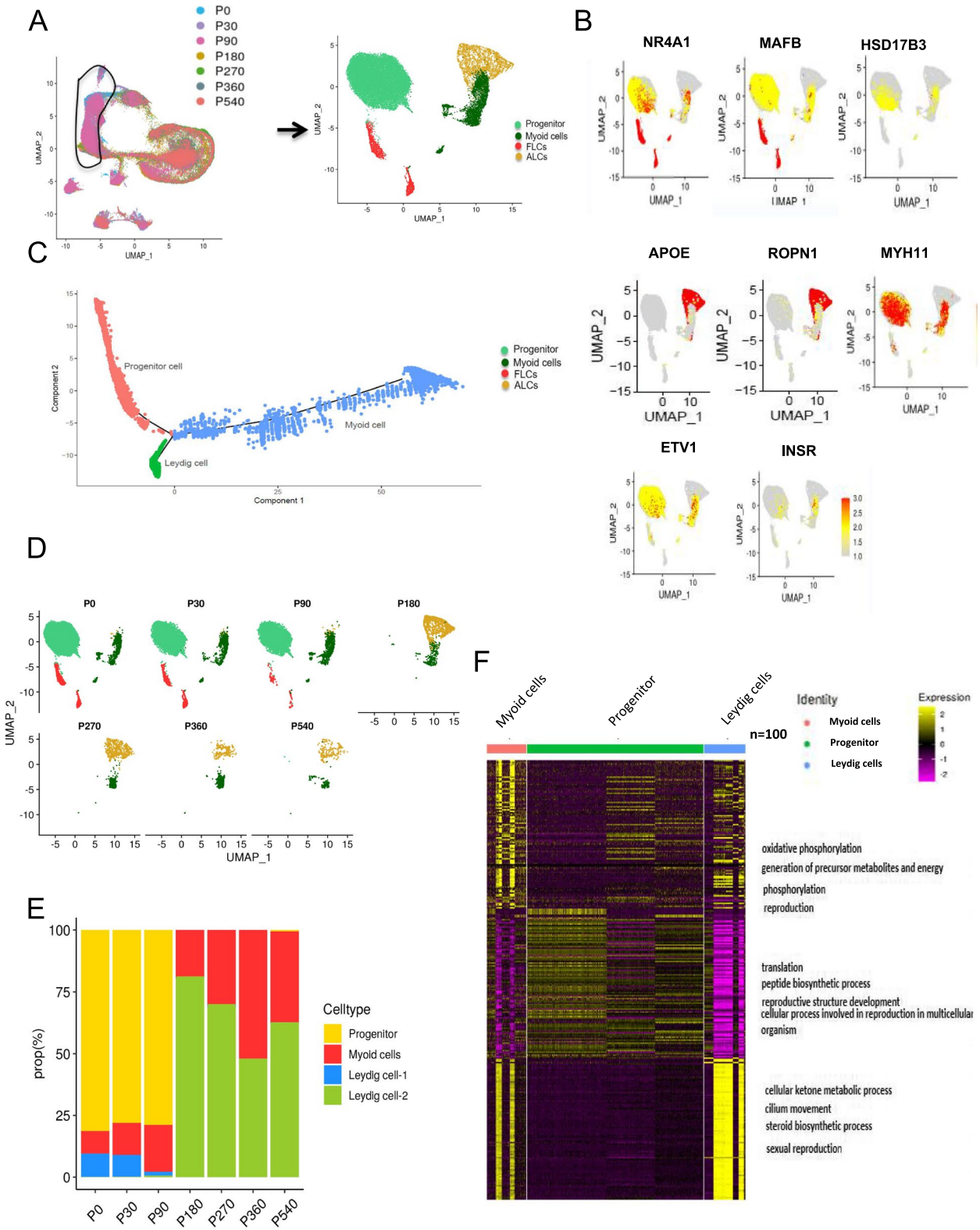

Fig. 5 Leydig and peritubular myoid cells in Hu sheep testes. **A** Focused UMAP and clustering analysis of the Leydig cells. **B** Expression patterns of representative markers projected onto the UMAP. **C** UMAP and clustering analysis of single-cell transcriptome data from Leydig cells of Hu sheep testes at different developmental stages. **D** Relative proportions of four Leydig cell subtypes in the testes of Hu sheep at different developmental stages. **E** Heatmap of 100 genes that exhibited dramatic changes in gene expression along the Leydig and myoid cell lineages. Representative GO terms and *P* values are shown for each cell type

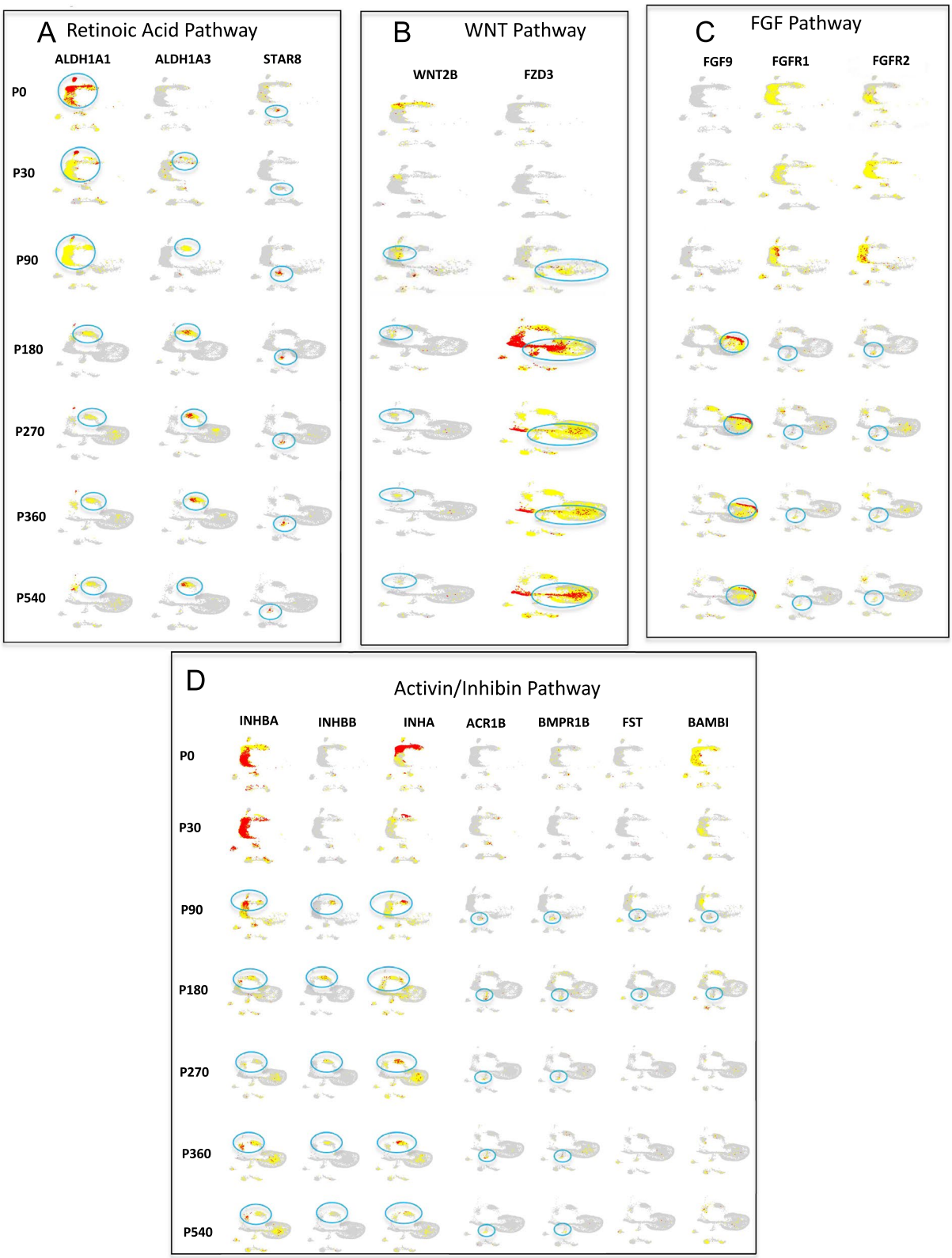

Fig. 6 Overview of the key signaling pathways regulating testes development. Relative expression levels of representative genes from RA, activin/inhibin, FGF, and WNT pathways projected onto the UMAP

Discussion

The testes are vital male reproductive organs with three functional cell classes: spermatogonia, spermatogenic cells, and supportive somatic cells [21]. Testicular development is driven by well-ordered and sequential changes in gene regulation and cellular organization, with the aim of maintaining a pool of cells that are able to give rise to male gametes throughout the male lifetime [22, 23]. However, little is known about the development of testicular cell lineages from the newborn to adult stage in sheep. Recently, scRNA-seq techniques have been applied to analyze spermatogenesis [18, 21, 24, 25]. Here, we aimed to provide foundational scRNA-seq data of all cells contained in the Hu sheep testes from birth to adulthood, complemented by computational analysis and validation studies, to offer new insights into the regulation of male gametogenesis.

At a broad level, we investigated the heterogeneity of Hu sheep testicular tissue and identified characteristic genes with expression specific to each cluster, which enabled us to deduce the corresponding cell types. Then, by analyzing 100,000 cells collected at time points from birth to adulthood, we identified the main germ cell types and somatic cell types in the sheep testes. Our study not only clarified the cell types in Hu sheep testicular tissue from birth to adulthood, but also revealed the dynamics of gene expression during spermatogenesis.

While the initial analysis of all the cells identified spermatogonial cells, it did not clearly distinguish the spermatogonial subtypes. However, by focused reclustering of spermatogonial cells and the use of marker genes defined in humans and mice, we were able to resolve undifferentiated and differentiated spermatogonia. Previous studies have defined four subtypes of spermatogonia in the mouse testes: undifferentiated spermatogonia (spermatogonia1, or SPG1) and three subtypes of differentiated spermatogonia (SPG2–4) [13]. In contrast to those in mice, spermatogonia in humans divide to form undifferentiated spermatogonia (SSC-1 and SSC-2), early differentiating (diff) SPG (early diff-SPG), and diff-SPG [7]. In this study, we show for the first time that sheep testicular spermatogonia can be divided into undifferentiated and differentiated spermatogonia. We observed a large increase in the proportion of spermatogonia from 3.2% at 0 day to 12.3% at 180 days and stabilization of this proportion thereafter. A similar increase has been previously documented in IF studies examining the relative number of undifferentiated spermatogonia [26, 27]. Notably, differentiated spermatogonia in Hu sheep testes appeared before tubule morphogenesis (that is, the appearance of a defined basal lamina and lumen), which is consistent with previous findings in pigs [27].

Previous studies usually classified Sertoli cells into two developmental stages: the immature stage and the mature stage [28, 29]. A recent scRNA-seq study on the testes before and after puberty proposed that there are two immature Sertoli cell states that eventually converge into a single mature state [28]. However, in this study, we observed a new phenomenon: with increasing age, the ratio between Immature Sertoli_1 and Immature Sertoli_2 cells decreases significantly, which indicates a dynamic transition in the process of Sertoli cell maturation. Through Venn diagram analysis, we identified 709 genes that are specifically expressed in Immature Sertoli_2 cells at 0, 30, and 90 days. The expression of these genes at early stages suggests they may play a crucial role during the neonatal period, influencing the determination and expansion of the Sertoli cell population and laying the groundwork for subsequent testicular functional maturation. We performed differential expression and GO enrichment analyses on these genes, confirming their involvement in several key biological processes. The enrichment in translation indicates that these genes are involved in protein synthesis, which is essential for the development of Sertoli cells. Their association with cell cycle processes (such as mitotic cell cycle and sister chromatid separation) demonstrates their role in cell division, potentially promoting the proliferation of Immature Sertoli_2 cells. Furthermore, their enrichment in the negative regulation of the cell cycle implies that they may be part of a regulatory mechanism that facilitates the transition from an immature to a mature state by halting or slowing down cell division as Sertoli cells mature. These findings are consistent with the functional changes of Sertoli cells across different developmental stages. Around puberty, Sertoli cells transition from a proliferative state to a mature state, and dynamic changes in gene expression during this process are critical for maintaining normal spermatogenesis. Around puberty, mature Sertoli cells are predominant, and their numbers become fixed and unmodifiable, a finding that is consistent with prior work [30, 31]. Our results also revealed that the specific marker genes of immature 1 and immature 2 differ. It is generally accepted that Sertoli cells proliferate during the fetal and neonatal periods but not after puberty. However, some research has shown either a residual capacity of adult Sertoli cells to proliferate or the long-term presence of some Sertoli cell precursors in the testes of adult seasonal breeders [31–33]. Our results demonstrate the persistence of Sertoli cell precursors and their ability to divide in sheep testes, consistent with previous findings in other species. The number of mature Sertoli cells may be maintained through progenitor cell division after the loss of proliferation ability.

At least two distinct Leydig cell populations emerge in sequence in the mammalian testes: FLCs and ALCs in the fetal and adult testes, respectively [34]. Importantly, the fate of FLCs in the postnatal period is the subject of debate. Cell lineage tracing analysis has shown that FLCs persist in the testes after birth, at least in mice [35]. Our results indicate that one type of Leydig cell is present in the Hu sheep testes after birth and is replaced by another type of Leydig cell after sexual maturity. We presume that the Leydig cells observed after birth are FLCs, while those observed after sexual maturity are ALCs. Our results confirmed that, similar to the case in mice, FLC numbers peak at birth, gradually decline and subsequently disappear during prepubertal life in Hu sheep. During pubertal testicular maturation, a second population, known as ALCs, differentiate and colonize the testicular interstitium to support male fertility throughout adulthood [36–38]. Analysis of Leydig and myoid cells revealed that these two types of cells differentiate from common progenitor cells, as also reported by Yu et al. in 2021. Furthermore, our results revealed that myoid cells, fetal Leydig cells, and precursors were present in the Hu sheep testes after birth. Previous studies have suggested that the ALCs population is derived not from the proliferation/differentiation of fetal Leydig cells present in the neonatal testes but from mesenchymal-like cells [39]. In this study of Hu sheep, the precursor cell type after birth may have been mesenchymal-like cells, which were subsequently transformed into ALCs, while the FLCs gradually disappeared with testes development.

Spermatogenesis is a complex process that is controlled by interactions between germ cells and somatic cells. To date, several signaling pathways have been found to be closely related to spermatogenesis in humans and mice [40–45]. We found that the RA pathway plays an important role in the transport of spermatogonia to spermatocytes after birth in Hu sheep, the WNT and activin/inhibin pathways begin to play a role before puberty, and the FGF pathway begins to play a role after sexual maturity. In general, different signaling pathways synergistically affect testicular development at different developmental stages.

Previous studies used scRNA-seq to study spermatogenesis in the testes of 1.5-year-old Hu sheep and identified five types of germ cells (early primary spermatocytes, late primary spermatocytes, round spermatids, elongated spermatids, and sperm) and two types of somatic cells (Sertoli cells and Leydig cells), but no spermatogonial cells were identified [46]. Wu et al. used the scRNA-seq technology to study Hu sheep testes at pre-sexual maturity stage (3 month old) [22]. Five male germ cell types (including two types of undifferentiated spermatogonia (A_{pale} and A_{dark}), primary spermatocytes, secondary spermatocytes, and sperm cells) and nine testicular somatic cell types (Sertoli cells, myoid cells, monocytes, macrophages, Leydig cells, dendritic cells, endothelial cells, smooth muscle cells, and leukocytes) were observed. A_{pale} and A_{dark} were found to be two distinct states of undifferentiated spermatogonia. In our study, we used scRNA-seq to construct a comprehensive transcriptional atlas of testes development at seven different developmental stages of Hu sheep from birth to adulthood. Seven testicular somatic cell types (Sertoli cells, myoid cells, macrophages, Leydig cells, endothelial cells, VSM, and T cells) and five germ cell types were clustered, and the marker genes of each type were also identified in Hu sheep testes. At birth, the germ cells are undifferentiated spermatogonia. By 30 days, differentiated spermatogonia can be observed. At 90 days, spermatocytes can be observed. Finally, at 180 days, a large number of spermatids emerge in the seminiferous tubules. Sertoli cells exhibit two distinct states before converging to a mature population during puberty, and that we identified a common progenitor for Leydig and myoid cells, with Leydig cells undergoing phased transition through progenitor and immature stages before reaching the terminally differentiated adult stage. The dynamic transcription map of Hu sheep testes provides a variety of insights into the developmental changes, the key factors and signaling pathways at different developmental stages of Hu sheep testes.

Our research is based on scRNA-seq data of testicular cells collected before and after puberty. Although this type of data source provides a wealth of information, it has certain limitations, as it may not fully represent all possible states of testicular cells or different genetic backgrounds, and this may affect our understanding of gene expression changes during the development of testicular cells. In addition, during the scRNA-seq process, we face several limitations, including insufficient sequencing depth, which may fail to capture low-abundance transcripts, thereby leading to an incomplete presentation of the transcriptome. The clustering algorithms that we use to distinguish different types of testicular cells are based on certain assumptions about data distribution, which may not fully correspond to actual biological differences, potentially leading to misclassification of cell states and thereby affecting the accurate understanding of cellular heterogeneity within the testis. Although strict statistical methods were used in the differential gene expression analysis, there is always the risk of false positives, i.e., some genes may be incorrectly identified as differentially expressed, which in turn affects the interpretation of gene functions and biological processes. To address these issues, future improvements may include increasing sequencing depth, employing advanced library

preparation techniques for a more comprehensive transcriptome, applying normalization methods that account for PCR bias to enhance the accuracy of gene expression quantification, exploring more robust clustering algorithms based on biological information, and implementing multiple statistical tests and validation methods in differential gene expression analysis. By integrating these improvement measures and continuously optimizing experimental procedures and analytical methods, we aim to enhance our understanding of testicular cell development. We also hope to provide more reliable data and conclusions for research in related fields.

In-depth study of the molecular mechanisms regulating sheep testicular development and spermatogenesis can accurately identify the major genes and signaling pathways that affect the spermatogenesis and thus fertility of sheep. Molecular breeding methods such as gene modification, gene knockout, and other genetic engineering technologies can be adopted to improve the fertility of offspring in the process of sheep breeding or variety improvement.

Conclusions

In conclusion, our comprehensive, whole-transcriptome scRNA-seq analyses revealed the major cell types in the sheep testes and the processes underlying their maturation. Our findings not only offer valuable knowledge concerning testicular development in mammals but also pave the way for understanding germ cell development and germ cell–niche communication.

Methods

Hu sheep husbandry and testes isolation

The experiments performed in this study were approved by the Animal Care and Use Committee of Inner Mongolia Agricultural University (License No. IMGND, 2020–0017). Hu sheep were housed and fed at Aowoteke Animal Husbandry Technology Co., Ltd., Chifeng, China. Prior to sampling, the Hu sheep were fasted for 12 h in order to minimize discomfort during the collection of testes. On days 0, 30, 90, 180, 270, 360, and 540, procaine hydrochloride injections were administered around the testes of the Hu sheep at dosages of 1 mL, 2 mL, 4 mL, 6 mL, 8 mL, 10 mL, and 12 mL, respectively. Three Hu sheep were selected for castration at each of these seven time points. Fresh testes were collected, washed with Dulbecco's phosphate-buffered saline (DPBS). The tissues were stored on ice and transported to the research laboratory within 40 min of removal. The tunica albuginea was dissected from each testis, and the entire testis was divided into smaller segments for subsequent processing.

Histological analysis

Samples of sheep testis tissue (1 cm^3) were collected, washed with DPBS to remove any external contaminants. Subsequently, they were fixed with 4% paraformaldehyde (PFA) for precisely 24 h at room temperature. After that, the samples underwent dehydration using a series of gradient alcohol concentrations (e.g., 70%, 80%, 90%, and 100%) to gradually remove water. Next, they were made transparent with xylene, a common clearing agent. Following this, the samples were immersed in melted paraffin at an appropriate temperature to infiltrate the tissue. Finally, the samples were embedded in paraffin blocks for sectioning. Four- to six-micron-thick sections were cut and stained with hematoxylin and eosin for histological analysis. The testis morphology was observed via a microscope (Nikon).

Immunostaining of testicular tissues

Sections were deparaffinized with xylene and rehydrated through an ethanol series (100%, 95%, 70%, 50%, water). They were then incubated in sodium citrate buffer (pH 6.0, 98 °C) for 30 min for antigen retrieval. Tissues were blocked with 5% normal donkey serum and incubated with primary antibodies (Additional file 14) overnight at 4 °C. The specificity of antibodies (UTF1, UCHL1, SYCP3, PIWIL4, TKTL1, HELLS, SOX9, AR, and AMH) was confirmed through peptide blocking assays (Additional file 9). The antibody alone, as well as the mixture of blocking peptide and the primary antibody (1:20 mass ratio), was used for comparison. The next day, sections were washed with DPBS and incubated with secondary antibodies for 2 h at room temperature. For IF, Alexa Fluor 555-conjugated goat anti-rabbit IgG H&L (1:200 dilution, BS-0295G-AF555; Bioss, China, Beijing) and goat anti-rabbit IgG H&L/FITC antibody (1:200 dilution, bs-0295G-FITC; Bioss, China, Beijing) were used. Sections were counterstained with DAPI for 10 min and using a confocal laser microscope (LSM, Zeiss, Oberkochen, Germany). The specificity of the primary antibodies was confirmed through peptide blocking assays (Additional file 15: Fig. S7).

Testes sample preparation for scRNA-seq

The testes were washed four times in DPBS (Gibco, Waltham, MA, USA), and the white testicular membrane tissues were removed. A 1-cm^3 piece of testicular tissue was cut, washed five times with DPBS, and then placed in a 1.5-mL centrifuge tube. The cleaned tissue samples were then digested in dissociation buffer containing 10 mg/mL collagenase IV for 10 min at 37 °C with gentle agitation, and the tubules were sedimented by centrifugation at 1200 rpm for 5 min. The precipitate was

subsequently digested in 10 mL of medium containing 5 mL of 500 μg/mL DNase and 5 mL of 0.25% trypsin/ethylenediaminetetraacetic acid (EDTA) for 15 min at 37 °C with vigorous mixing. The digestion was then terminated by adding fetal bovine serum. The cell suspension was mixed to homogeneity and then filtered through 40-μm screens successively. The filtrate was collected and centrifuged at 300 × g at 4 °C for 5 min. After the supernatant was discarded, the cells were resuspended in DPBS. A total of 10 μL of cell suspension and 10 μL of acridine orange/propidium iodide (AO/PI) were added to a new RNase-free centrifuge tube and gently mixed. Then, 20 μL of this solution was added to a Countstar® cell counting plate and analyzed using a Countstar® Rigel S2 cell analyzer to record the cell concentration and viability. Cells with a viability > 90% were adjusted to 1000 cells/μL for a scRNA-seq.

10 × Genomics scRNA-seq

The scRNA-seq libraries were prepared using a Single Cell 3' Library Gel Bead Kit V2 (10 × Genomics, 120237) following the manufacturer's instructions. In brief, single cells were loaded onto a 10 × Genomics to generate single-cell gel beads in emulsion (GEMs) using the Single Cell 3' Library and Gel Bead Kit V2 (10 × Genomics, 120237). Captured cells were lysed and subjected to RNA barcoding through reverse transcription in individual GEMs. Barcoded cDNAs were pooled and cleaned using beads (Invitrogen, 37002D). Paired-end sequencing (150 bp) was performed on an Illumina HiSeq X Ten instrument.

Sequencing data processing

Raw gene expression matrices were generated for each sample via the Cell Ranger (v6.1.2) pipeline coupled with the *Ovis aries* reference Oar_rambouillet_v1.0. The output filtered gene expression matrices were analyzed in R software (version 4.3.1) with the Seurat package (version 4.3.0.1). A custom R script was used to combine the expression data and metadata from all the libraries corresponding to a single batch. The expression data matrix was then loaded into a Seurat object along with the library metadata for downstream processing. The percentage of mitochondrial transcripts for each cell (percent.mt) was calculated and added as metadata to the Seurat object. The cells were further filtered before dimensionality reduction according to the following parameters: nFeature_RNA-min. 500; percent.mt-max. 20%. The expression values were then scaled to 10,000 transcripts per cell and log-transformed (NormalizeData function, normalization.method = "LogNormalize", scale.factor = 10,000). We calculated the variable features via the FindVariableFeatures function with selection.method = "vst" and nfeatures = 2000. The effects of variables (percent.mt) were estimated and regressed out using the ScaleData function (vars.to.regress = "percent.mt"), and the scaled and centered residuals were used for dimensionality reduction and clustering. The code and scripts used for the analysis are provided in the supplementary files.

Dimensionality reduction

To reduce the dimensionality of the dataset, the RunPCA function was used with default parameters on the linear-transformation scaled data generated by the ScaleData function. To allow the combination of cells from different samples, we used the RunHarmony (Harmony2, v0.1.1) function to correct for batch effects. The ElbowPlot function was used to determine the appropriate number of dimensions for the dataset (first 30 PCs).

Cell clustering and cluster identification

We applied the FindNeighbors function prior to clustering; this function takes as input the previously defined dimensionality of the dataset (first 30 PCs). Clustering was performed using the FindClusters function with a resolution parameter of 0.3. After nonlinear dimensional reduction, all the cells were projected into two-dimensional space via UMAP. Clusters were assigned preliminary identities on the basis of the expression of combinations of known marker genes of major cell classes and types.

Cell cycle analysis

We performed cell cycle analysis via the "CellCycleScoring" function in Seurat. Scores were assigned to cells on the basis of the expression of genes associated with the G1, S, or G2/M phase. The quantification of cells in each phase was performed via the "Prop.table" function.

Differentially expressed gene (DEG) identification

Differentially expressed genes were identified using the FindAllMarkers function in Seurat with parameter only.pos = TRUE. DEGs were filtered using a maximal *P* value of 0.05.

Pseudotime analysis by Monocle

Trajectory inference was performed using Monocle version 2.28.0 with the parameters recommended by the developers. First, the raw count data from the Seurat object were converted to a CellDataSet object via the newCellDataSet function in Monocle. Second, the

differentialGeneTest function (cut-off of $q < 0.01$) was applied to identify variable genes, and then the top 5000 most significant genes were set as the ordering genes via the setOrderingFilter function. Finally, we used the reduceDimension function (reduction_method = "DDRTree") to reduce the space to two dimensions. The visualization function plot_cell_trajectory function was applied to the ordered cells to plot each group along the same pseudotime trajectory.

Enrichment analysis

DEGs were sorted based on their average log2 fold change (avg_log2FC). We selected the top 100 cluster DEGs from each cluster for GO and KEGG enrichment analysis. The enrichment analysis was conducted using the clusterProfiler R package (version 4.8.1). For the enrichment analysis of DEGs between groups, we selected DEGs with P value < 0.05, avg_log2FC > log2(1.5), and a percentage of cells expressing the gene in at least one group (pct.1) > 0.25.

Statistical analysis

A nonparametric Wilcoxon rank sum test was used to analyze the differential gene expression between the two groups. All statistical analyses were performed in R or GraphPad Prism (version 8.0). Results were considered statistically significant at $P < 0.05$.

Abbreviations

ALCs	Adult Leydig cells
AO	Acridine orange
DPBS	Dulbecco's phosphate-buffered saline
EDTA	Ethylenediaminetetraacetic acid
FLCs	Fetal Leydig cells
GEMs	Gel beads in emulsion
Genomics	Chromium Single Cell Controller
GO	Gene Ontology
PI	Propidium iodide
RA	Retinoic acid
scRNA-seq	Single-cell RNA sequencing
SSCs	Spermatogonial stem cells
t-SNE	T-distributed Stochastic Neighbor Embedding
UMAP	Uniform manifold approximation and projection
VSM	Vascular smooth muscle cell
VWF	Von Willebrand factor

Supplementary Information

The online version contains supplementary material available at https://doi.org/10.1186/s12915-025-02186-y.

Additional file 1: Supplementary Fig. S1 scRNA-seq workflow.

Additional file 2: Supplementary Table S1 Analysis code and scripts.

Additional file 3: Supplementary Table S2 scRNA-seq information.

Additional file 4: Supplementary Fig. 2 Gene expression patterns of additional markers of niche/somatic cells, projected onto the t-distributed Stochastic Neighbor Embedding (t-SNE) plot.

Additional file 5: Supplementary Fig. 3 Analysis of testicular differential genes in different developmental stages of Hu sheep.

Additional file 6: Supplementary Fig. 4 H&E staining of Hu sheep testes sections from different developmental stages. Scale bar = 20 μm.

Additional file 7: Supplementary Fig. 5 Distinct phase of spermatogonial proliferation and differentiation from birth to adulthood in Hu sheep testes. (A) Bar chart showing the relative proportion of different cell types for each age. (B) IF for UCHL1$^+$ cells and KIT$^+$ cells in Hu sheep testes during different developmental stages. Scale bar = 20 μm. (C) IF for UCHL1$^+$ cells and PCNA$^+$ cells in Hu sheep testes during different developmental stages. Scale bar = 20 μm. (D) IF for SYCP3$^+$ cells and VASA$^+$ cells in Hu sheep testes during different developmental stages. Scale bar = 20 μm.

Additional file 8: Supplementary Table S3 Germ cell differentially expressed genes.

Additional file 9: Supplementary Table S4 Top 10 differentially expressed genes in testicular germ cells of Hu sheep.

Additional file 10: Supplementary Table S5 GO analysis of the DEGs for germ cell populations.

Additional file 11: Supplementary Fig. 6 Identification of Sertoli states in Hu sheep testes. (A) UMAP and clustering analysis of single cell transcriptome data from Sertoli cells of Hu sheep testes at different developmental stages. (B) Gene expression patterns of additional markers of niche/somatic cells, projected onto the t-SNE plot. (C) Relative proportion of three Sertoli cells in testes of Hu sheep at different developmental stages. (D) Immunofluorescence for SOX9$^+$ cells and PCNA$^+$ cells in Hu sheep testes during different developmental stages. Scale bar = 50 μm. (E) Venn diagram of differential genes immature Sertoli cells 1 and 2 and mature Sertoli cells. (F) Heatmap of 100 genes that exhibited dramatic changes in gene expression at the intersection of two consecutive stages of Sertoli cell development. Representative GO terms and *P* values are shown for each cell type.

Additional file 12: Supplementary Table S6 Genes differentially expressed in immature Sertoli cells 1 and 2 and mature Sertoli cells.

Additional file 13: Supplementary Table S7 GO analysis of the DEGs for immature Sertoli cells 1 and 2 and mature Sertoli cells.

Additional file 14: Supplementary Table S8 Antibodies list.

Additional file 15: Supplementary Fig. 7 The specificity of primary antibodies is confirmed through peptide blocking assays. (A) The specificity of primary antibody UCHL1 is confirmed through peptide blocking assays. (B) The specificity of primary antibody SYCP3 is confirmed through peptide blocking assays. (C) The specificity of primary antibody UTF1 is confirmed through peptide blocking assays. (D) The specificity of primary antibody TKTL1 is confirmed through peptide blocking assays. (E) The specificity of primary antibody PIWIL1 is confirmed through peptide blocking assays. (F) The specificity of primary antibody HELLS is confirmed through peptide blocking assays. (G) The specificity of primary antibody SOX9 is confirmed through peptide blocking assays. (H) The specificity of primary antibody AMH is confirmed through peptide blocking assays. (I) The specificity of primary antibody AR is confirmed through peptide blocking assays. Positive control staining (A1, B1, C1, D1, E1, F1, G1, H1, I1) and corresponding blocking peptide results (A2, B2, C2, D2, E2, F2, G2, H2, I2). Scale bar: 50 μm.

Acknowledgements

We thank Aowoteke Animal Husbandry Technology Co., Ltd. (Chifeng, Inner Mongolia, China) for providing the experimental animals.

Authors' contributions

GFC and YLS designed the research; JS performed the IF research and wrote the original manuscript; YYY and HS performed the H&E staining; FFZ, DQW, BS, and CC analyzed the data; CQZ, MZ, XNL, and TYH produced the figures. YT and XHL revised manuscript. The authors read and approved the final manuscript.

Funding
This study was supported by Science and Technology Planning Project of Inner Mongolia (No. 2020CG0078; No. 2021GG0062) and Introduction Project of High-Level Talents in Biology (to Song Yongli, No. 10000–22120301/011).

Data availability
All data generated or analyzed during this study are included in this published article, its supplementary information files, and publicly available repositories. The data have been deposited in the Sequence Read Archive [BioProject: PRJNA865464] (https://www.ncbi.nlm.nih.gov/bioproject/?term=PRJNA865464).

Declarations

Ethics approval and consent to participate
All sheep experimental procedures and protocols used in this study were approved and authorized by the animal care and use committee of Inner Mongolia Agricultural University (License No. IMGND, 2020–0017).

Consent for publication
Not applicable.

Competing interests
The authors declare that they have no competing interests.

Received: 26 March 2024 Accepted: 5 March 2025
Published online: 12 March 2025

References

1. Kim H, Moon C, Shin T. Immunohistochemical study of flotillin-1 in the rat testis during postnatal development. Acta Histochem. 2008;110(3):224–31.
2. Murat F, Mbengue N, Winge SB, Trefzer T, Leushkin E, Sepp M, et al. The molecular evolution of spermatogenesis across mammals. Nature. 2023;613(7943):308–16.
3. Zhou R, Wu J, Liu B, Jiang Y, Chen W, Li J, et al. The roles and mechanisms of Leydig cells and myoid cells in regulating spermatogenesis. Cell Mol Life Sci. 2019;76(14):2681–95.
4. Griswold MD. The central role of Sertoli cells in spermatogenesis. Semin Cell Dev Biol. 1998;9(4):411–6.
5. Shima Y, Miyabayashi K, Haraguchi S, Arakawa T, Otake H, Baba T, et al. Contribution of Leydig and Sertoli cells to testosterone production in mouse fetal testes. Mol Endocrinol. 2013;27(1):63–73.
6. Wang YQ, Chen SR, Liu YX. Selective deletion of WLS in peritubular myoid cells does not affect spermatogenesis or fertility in mice. Mol Reprod Dev. 2018;85(7):559–61.
7. Sohni A, Tan K, Song HW, Burow D, de Rooij DG, Laurent L, et al. The neonatal and adult human testis defined at the single-cell level. Cell Rep. 2019;26(6):1501-17.e4.
8. Lukassen S, Bosch E, Ekici AB, Winterpacht A. Single-cell RNA sequencing of adult mouse testes. Sci Data. 2018;5:180192.
9. Abid SN, Richardson TE, Powell HM, Jaichander P, Chaudhary J, Chapman KM, et al. A-single spermatogonia heterogeneity and cell cycles synchronize with rat seminiferous epithelium stages VIII-IX. Biol Reprod. 2014;90(2):32.
10. Bhushan S, Aslani F, Zhang Z, Sebastian T, Elsässer HP, Klug J. Isolation of Sertoli cells and peritubular cells from rat testes. J Vis Exp. 2016;108:e53389.
11. Guo J, Nie X, Giebler M, Mlcochova H, Wang Y, Grow EJ, et al. The dynamic transcriptional cell atlas of testis development during human puberty. Cell Stem Cell. 2020;26(2):262-76.e4.
12. Di Persio S, Neuhaus N. Human spermatogonial stem cells and their niche in male (in)fertility: novel concepts from single-cell RNA-sequencing. Hum Reprod. 2023;38(1):1–13.
13. Green CD, Ma Q, Manske GL, Shami AN, Zheng X, Marini S, et al. A comprehensive roadmap of murine spermatogenesis defined by single-cell RNA-seq. Dev Cell. 2018;46(5):651-67.e10.
14. Jiang Z, Wan Y, Li P, Xue Y, Cui W, Chen Q, et al. Effect of curcumin supplement in summer diet on blood metabolites, antioxidant status, immune response, and testicular gene expression in Hu sheep. Animals (Basel). 2019;9(10):720.
15. Yue GH. Reproductive characteristics of Chinese Hu sheep. Anim Reprod Sci. 1996;44(4):223–30.
16. Lukassen S, Bosch E, Ekici AB, Winterpacht A. Characterization of germ cell differentiation in the male mouse through single-cell RNA sequencing. Sci Rep. 2018;8(1):6521.
17. Zhang W, Xia S, Xiao W, Song Y, Tang L, Cao M, et al. A single-cell transcriptomic landscape of mouse testicular aging. J Adv Res. 2023;53:219–34.
18. Hermann BP, Cheng K, Singh A, Roa-De La Cruz L, Mutoji KN, Chen IC, et al. The mammalian spermatogenesis single-cell transcriptome, from spermatogonial stem cells to spermatids. Cell Rep. 2018;25(6):1650-67.e8.
19. Ernst C, Eling N, Martinez-Jimenez CP, Marioni JC, Odom DT. Staged developmental mapping and X chromosome transcriptional dynamics during mouse spermatogenesis. Nat Commun. 2019;10(1):1251.
20. Su J, Yang Y, Zhao F, Zhang Y, Su H, Wang D, et al. Study of spermatogenic and Sertoli cells in the Hu sheep testes at different developmental stages. Faseb j. 2023;37(8):e23084.
21. Lau X, Munusamy P, Ng MJ, Sangrithi M. Single-cell RNA sequencing of the cynomolgus macaque testis reveals conserved transcriptional profiles during mammalian spermatogenesis. Dev Cell. 2020;54(4):548-66.e7.
22. Wu Y, Guo T, Li J, Niu C, Sun W, Zhu S, et al. The transcriptional cell atlas of testis development in sheep at pre-sexual maturity. Curr Issues Mol Biol. 2022;44(2):483–97.
23. Faucette AN, Maher VA, Gutierrez MA, Jucker JM, Yates DC, Welsh TH Jr, et al. Temporal changes in histomorphology and gene expression in goat testes during postnatal development. J Anim Sci. 2014;92(10):4440–8.
24. Chen Y, Zheng Y, Gao Y, Lin Z, Yang S, Wang T, et al. Single-cell RNA-seq uncovers dynamic processes and critical regulators in mouse spermatogenesis. Cell Res. 2018;28(9):879–96.
25. Margolin G, Khil PP, Kim J, Bellani MA, Camerini-Otero RD. Integrated transcriptome analysis of mouse spermatogenesis. BMC Genomics. 2014;15:39.
26. Ren F, Xi H, Qiao P, Li Y, Xian M, Zhu D, et al. Single-cell transcriptomics reveals male germ cells and Sertoli cells developmental patterns in dairy goats. Front Cell Dev Biol. 2022;10:944325.
27. Almunia J, Nakamura K, Murakami M, Takashima S, Takasu M. Characterization of domestic pig spermatogenesis using spermatogonial stem cell markers in the early months of life. Theriogenology. 2018;107:154–61.
28. Yu XW, Li TT, Du XM, Shen QY, Zhang MF, Wei YD, et al. Single-cell RNA sequencing reveals atlas of dairy goat testis cells. Zool Res. 2021;42(4):401–5.
29. Meroni SB, Galardo MN, Rindone G, Gorga A, Riera MF, Cigorraga SB. Molecular mechanisms and signaling pathways involved in Sertoli cell proliferation. Front Endocrinol (Lausanne). 2019;10:224.
30. Orth JM, Gunsalus GL, Lamperti AA. Evidence from Sertoli cell-depleted rats indicates that spermatid number in adults depends on numbers of Sertoli cells produced during perinatal development. Endocrinology. 1988;122(3):787–94.
31. Sharpe RM, McKinnell C, Kivlin C, Fisher JS. Proliferation and functional maturation of Sertoli cells, and their relevance to disorders of testis function in adulthood. Reproduction. 2003;125(6):769–84.
32. Johnson L, Varner DD, Tatum ME, Scrutchfield WL. Season but not age affects Sertoli cell number in adult stallions. Biol Reprod. 1991;45(3):404–10.
33. Tarulli GA, Stanton PG, Lerchl A, Meachem SJ. Adult sertoli cells are not terminally differentiated in the Djungarian hamster: effect of FSH on proliferation and junction protein organization. Biol Reprod. 2006;74(5):798–806.
34. Roosen-Runge EC, Anderson D. The development of the interstitial cells in the testis of the albino rat. Acta Anat (Basel). 1959;37:125–37.
35. Kaftanovskaya EM, Lopez C, Ferguson L, Myhr C, Agoulnik AI. Genetic ablation of androgen receptor signaling in fetal Leydig cell lineage affects Leydig cell functions in adult testis. Faseb j. 2015;29(6):2327–37.
36. Habert R, Lejeune H, Saez JM. Origin, differentiation and regulation of fetal and adult Leydig cells. Mol Cell Endocrinol. 2001;179(1–2):47–74.
37. Haider SG. Cell biology of Leydig cells in the testis. Int Rev Cytol. 2004;233:181–241.
38. Teerds KJ, Huhtaniemi IT. Morphological and functional maturation of Leydig cells: from rodent models to primates. Hum Reprod Update. 2015;21(3):310–28.
39. Benton L, Shan LX, Hardy MP. Differentiation of adult Leydig cells. J Steroid Biochem Mol Biol. 1995;53(1–6):61–8.
40. Zhang HZ, Hao SL, Yang WX. How does retinoic acid (RA) signaling pathway regulate spermatogenesis? Histol Histopathol. 2022;37(11):1053–64.

41. Khanehzad M, Abbaszadeh R, Holakuyee M, Modarressi MH, Nourashrafeddin SM. FSH regulates RA signaling to commit spermatogonia into differentiation pathway and meiosis. Reprod Biol Endocrinol. 2021;19(1):4.
42. Ferder IC, Fung L, Ohguchi Y, Zhang X, Lassen KG, Capen D, et al. Meiotic gatekeeper STRA8 suppresses autophagy by repressing Nr1d1 expression during spermatogenesis in mice. PLoS Genet. 2019;15(5):e1008084.
43. Anderson EL, Baltus AE, Roepers-Gajadien HL, Hassold TJ, de Rooij DG, van Pelt AM, et al. Stra8 and its inducer, retinoic acid, regulate meiotic initiation in both spermatogenesis and oogenesis in mice. Proc Natl Acad Sci U S A. 2008;105(39):14976–80.
44. Bläuer M, Husgafvel S, Syvälä H, Tuohimaa P, Ylikomi T. Identification of a nuclear localization signal in activin/inhibin betaA subunit; intranuclear betaA in rat spermatogenic cells. Biol Reprod. 1999;60(3):588–93.
45. Nakajima S, Hayashi M, Kouguchi T, Yamaguchi K, Miwa M, Yoshizaki G. Expression patterns of gdnf and gfrα1 in rainbow trout testis. Gene Expr Patterns. 2014;14(2):111–20.
46. Yang H, Ma J, Wan Z, Wang Q, Wang Z, Zhao J, et al. Characterization of sheep spermatogenesis through single-cell RNA sequencing. Faseb J. 2021;35(2):e21187.

Publisher's Note